Initial Cost Considerations on the Use of Fibre Reinforced Plastics in Reinforced Concrete Structures

Ioannis Balafas[1], Chris Burgoyne[1]

ABSTRACT: Research on the use of fibre reinforced plastics (FRPs) in concrete structures, as an alternative to steel, dates back to the 1970s. The driving force has been the inability of steel to cope with corrosion in aggressive environments. FRPs are recognised as an alternative for several structural applications, but they are rejected due to their high initial cost. To date, most applications have been to demonstration structures. A corollary is that the composites industry hesitates to invest in materials designed for structural engineering due to limited demand. Because of the high initial cost of FRPs, optimum use of their properties should be made in design. This paper focuses on the economics of reinforced concrete (RC) structures using either steel or FRP as main reinforcement. A method to select optimum structural dimensions with respect to cost is presented, and the parameters affecting the design solutions are identified. Comparisons with steel alternatives are made. It was found that in contrast to steel, the working load conditions govern FRP design. But for the most economic solutions engineers have to take account of the ultimate conditions in their calculations to control brittle snapping of FRP before concrete crushing at failure.

INTRODUCTION

One of the obstacles to adopting fibre reinforced plastic (FRP) reinforcement in concrete structures is their initial high cost compared to their metal competitors. Numerous structures are deteriorating due to harsh environmental conditions and extensive use of de-icing salts. In North America corrosion is extensive in parking garages and bridge decks. In Canada the estimated cost of repairing parking garages is in the range of $6 billion (US) (Bedard, 1992). The expected cost of repairing existing highway bridges in USA is over $80 billion and between $1 and $3 trillion for all concrete structures (Fickelhorn, 1990). Corrosion problems also exist in Arabian Gulf countries. Deterioration of all types of structures is observed, due to high concentrations of chlorides in construction materials, high humidity and marine atmosphere (Makhtouf, 1991). These numbers are expected to increase substantially in the future.

Due to FRPs' high tensile strength, most structural applications with reinforced concrete use the FRP as tension reinforcement in beam-like structures. For this study a structure was chosen and the design constraints were identified. By varying the depth of the section and the area of reinforcement, several design solutions can be found. If those solutions are plotted on a depth versus bar area diagram a feasible zone is created. By introducing a costing function in the graph the most economic structures can be found. Alsayed and Al-Salloum (Alsayed et al., 1996) used a similar approach. Here, more design constraints and more accurate formulas are used, as well as analysing the structure in a different way.

The intention of this work is to give practicing engineers a better feel for FRP cost-design interaction and to identify where further research is needed, pushing design solutions to more economic fields.

[1] Engineering Department, Cambridge University

STRUCTURE SELECTION

A simply supported beam was chosen for the analysis. One of the drawbacks in the design with FRPs is their brittle nature. Plastic behaviour gives warning and moment redistribution can be achieved in indeterminate structures before failure. In a typical determinate steel RC beam, large deformations tend to develop very quickly with a small increase of load due to yielding of steel. Thus for load control actions, warning before failure may come too late for remedial action. On the other hand, for displacement control actions, the structure can follow the load displacement curve, so it does not collapse at the maximum load, hence giving sufficient warning before failure. But in all cases, design should make sure that very brittle modes of failures such as snapping of the FRPs, which can lead to a catastrophic collapse, are eliminated.

In the absence of ductility, design methods based on equilibrium conditions, like the lower bound plasticity theory, cease to be valid or work only to a limited extent. The stress distribution assumed during design in these cases has to be correct. Methods based on compatibility, like the upper bound plasticity theory can still be valid (Heyman, 1982). Other methods for getting plastic behaviour in FRP reinforced structures is an active research topic.

Only the flexural mode of failure was considered in this study. Shear can be another mode of failure but the use of FRP as shear reinforcement is not effective due to its low stiffness, its lack of ductility and the effects on the strength of the corner radii (Yang et al., 2001). Existing methods of tackling shear such as the truss analogy or strut and tie models rely on lower bound plasticity theory which is not valid for brittle reinforcement (Stratford, 2000).

DESIGN CONSTRAINTS: ULTIMATE CONDITIONS

Moment capacity

The structure was loaded with a distributed load of $w=1.4G+1.6LL$, where G and LL are the dead load and live loads respectively. The critical moment at midspan is $wl^2/8$, where l is the span. Sectional analysis was performed (Figure 1) assuming:

1. Compatibility: plane sections remain plane. If ε_0 is the strain at centroid of the section then each point at the section has a strain of:

$$\varepsilon_x = \varepsilon_0 + \psi y \tag{1}$$

   where ψ is the curvature of the section and y the distance from the centroid (positive distance above the centroid and compressive strains).

2. Material law:
   - Concrete: rectangular block stress distribution over a length of 0.8 times the neutral axes depth. Failure strain 0.0035.
   - FRP: linear elastic up to failure.
   - Steel: linear elastic up to yielding point and strain hardening up to snapping, with a hardening slope of $(f_u-f_y)/(e_u-e_y)$, where (e_u, f_u), (e_y, f_y) are strain and stress values at max load and yielding load respectively.

3. Equilibrium: of forces and moments in the cross section.

Two modes of failure can occur at the ultimate load: crushing of concrete or reinforcement snapping. In the first case the concrete strain at the top fibre (ε_t, Fig. 1) was fixed as 0.0035. By assuming a reinforcement area, the two equations of equilibrium (force and moment) can be solved for beam depth and bottom fibre strain (ε_b, Fig. 1). If the bottom strain was greater than the snapping strain of the reinforcement the reinforcement snapping mode equilibrium system was activated. In that case the bar strains were fixed to values taken from Table 2 and the system was solved for top strain (ε_t) and section depth. Newton's method was used to solve the non-linear systems for a range of bar areas, from very low to very high reinforcement ratios. The results represent beams with same strength but different material proportions. Finally the results were plotted on a bar area versus depth graph and a feasible zone for that constraint was created (Figure 2).

Minimum and maximum reinforcement ratios

Minimum reinforcement ratios (p_{min}) represent beams with balanced concrete crushing and reinforcement snapping modes of failures. Accordingly, maximum reinforcement ratios (p_{max})

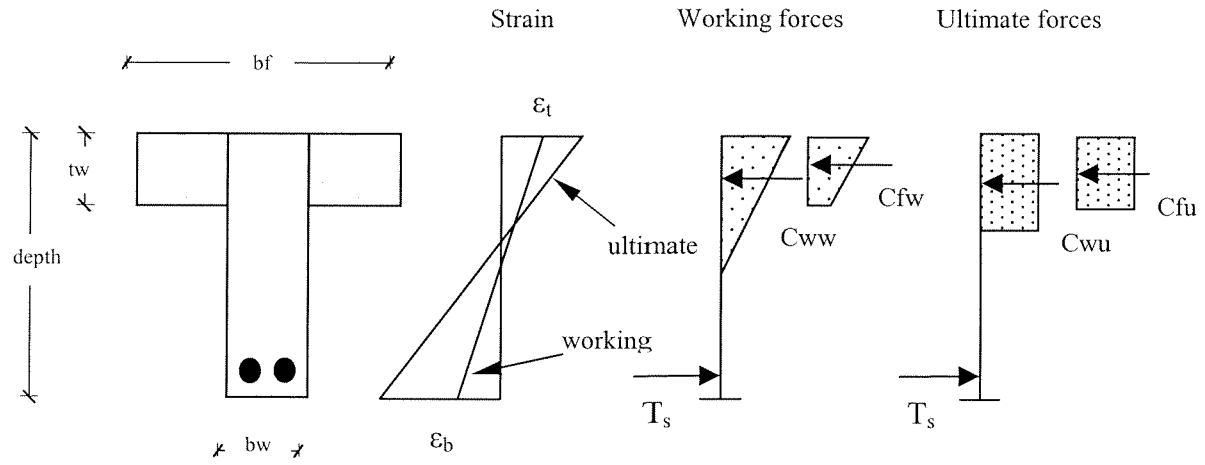

Figure 1: Working and ultimate sectional analysis

represent beams with balanced concrete crushing and bar yielding. The maximum reinforcement ratio values refer only to steel reinforced beams.

By assuming values of reinforcement areas, the top and bottom (ε_t, ε_b) strains were fixed to material failure strains and the equilibrium system was solved for depth and moment capacity.

DESIGN CONSTRAINTS: WORKING CONDITIONS

Deflections

For all working-load conditions linear elastic properties were assumed for concrete (Figure 1). Deflections can be found by integrating curvatures along the span while applying the theorem of virtual work. For a simply supported beam uniformly loaded without variations in the cross section or reinforcement ratio across span, the deflections can be given from:

$$\Delta = \frac{10}{96}\psi l^2 \qquad (2)$$

where l is the span.

In contrast to strength, deflections do not depend on the weak section but on the overall stiffness of the structure. So for a cracked beam the cracked and uncracked portions should be taken into consideration. All calculation methods are empirical, combining curvatures from uncracked and cracked regions. The two most widely used are the Branson formula, modified for FRP RC design (ACI 440-96, 1996), adopted mostly by the American codes, and the CEB formula (CEB, 1985). The CEB average curvature formula is used in this paper.

According to the CEB manual the average curvature of a cracked beam is given by:

$$\psi_m = (1-\varsigma)\psi_1 + (1-\varsigma)\psi_2 \tag{3}$$

where ψ_1, ψ_2 are the curvatures for state 1 (uncracked) and state 2 (cracked) respectively, and ζ is an interpolating coefficient which is given by:

$$\zeta = 1 - \beta_1\beta_2\left(\frac{\varepsilon_{sr}}{\varepsilon_{s2}}\right)^2 \tag{4}$$

where β_1 =1 and 0.5 for high bond and plain bars, respectively. β_2 =1 and 0.5 respectively for first loading and for loads applied in a sustained manner or for large number of load cycles. ε_{sr} is the reinforcement strain of the cracked section, when external moment is equal to the cracking moment and ε_{s2} the reinforcement strain for given external moment.

Equation (2) can be added to the equilibrium system described above in the section on the ultimate loads. In this case none of the materials fail, so strains were not fixed to a certain value. With the reinforcement area assumed there are now three unknown parameters: the top and bottom strain values (ε_t, ε_b) and the depth of the beam. They can be found by solving the three equations for force & moment equilibrium and deflection. The solutions represent structures which deflect equally for the given moment.

To calculate ε_{sr}, a sub-iteration was added to the principal 3 by 3 system iteration. In each iteration cycle, a subsystem was solved for the force-moment equilibrium of the same section loaded with its cracking moment for top and bottom strains (ε_t, ε_b). With known extreme fibre strains, using equation (1), the strain at the reinforcement level can also be found.

It should be noted here that in equation (4), (M_{cr}/M) can be used instead of $(\varepsilon_{sr}/\varepsilon_{s2})$ when the depth of the neutral axes is insensitive to loading. This assumption is realistic for reinforced but not for prestressed sections.

To account for creep effects, the elastic modulus of the concrete was set to:

$$E_{ct} = \frac{E_c}{1 + \varphi(t,t_0)\chi(t,t_0)} \tag{5}$$

where t_0 is the age at loading and t is the age for which strain or stress is calculated. φ is the known as creep coefficient and χ is the aging coefficient (Bazant, 1972) which allows for external loads developing gradually with time.

Shrinkage was considered in the calculations as a compressive strain induced at the centroidal level. Equilibrium redistributes those strains in the section.

Crack widths

The crack width depends on the bar strain, diameter and bond characteristics. To find the crack width a bond analysis is carried out (Stratford, 2000). By applying equilibrium and compatibility at a beam in bending and reinforced near the bottom fibres, one can come up with the well known bond equation, connecting the slip to the bond stress of the bar:

$$\frac{d^2 slip}{dx^2} = K\tau \tag{6}$$

where x is length and K a property of the section given from:

$$K = \frac{4}{\varphi E_p}\left[1 + \frac{n_f A_f E_p}{E_c}\left(\frac{1}{A} + \frac{e^2}{I}\right)\right] \tag{7}$$

φ is the bar diameter, E_p the reinforcement elastic modulus, η_f the number of bars at the cross section, A_f the area of each bar, E_c the concrete elastic modulus, e the eccentricity of the bars from the centroid, A, I the area and the second moment of area of the section.

To solve equation (6) a bond stress relationship should be assumed. The CEB model code (CEB, 1990) bond stress-slip relationship is assumed in this analysis:

Primary zone ($slip<s_1$): $\tau = p_1 slip^N$ (8)

Degradation zone ($s_1<slip<s_2$): $\tau = p_2 - p_3 slip$ (9)

Secondary zone ($slip<s_1$): $\tau = \tau_2$ (10)

p_1, p_2, p_3 are constant bond properties for the bars and usually measured through pull-out tests. Substituting (8), (9) and (10) into (6), three different boundary-value second-order differential equations are formed, which can be solved in a closed form for the working state (Stratford, 2000). The closed form solutions which are of interest in this work, are the one connecting the slip between concrete and reinforcement to the bar strains. If s_{ld} is the slip of the bar, along the debonding region, at a side of a crack, then the crack at that point will have a width:

$$w = 2\, s_{ld} \tag{21}$$

Going back to the section analysis, the bar strain is fixed to the value which produces the given crack width. The equilibrium system is solved for top fibre strains (ε_t) and depth, while the reinforcement area takes a range of values. The solutions represent structures which give a certain crack width when loaded with a given moment. The values are plotted on a bar area versus depth diagram and a feasible zone for this constraint is formed. In (7) η_f was found by dividing the total reinforcement area, used in the iterations, with the area of a certain type of bar A_f.

Concrete strain

Concrete in compression, at working conditions, has to take strains lower than a certain value. In this case the top fibre strain (ε_t) was fixed, and for a range of bar areas, the equilibrium system was solved for bottom strain (ε_b) and section depth.

CURVE FITTING

The design cases to be solved were, at the ultimate load, strength, p_{min} and p_{max}, while at the working load, deflections, crack width and compression strains. To assist with the optimisation calculation, spline curves were fitted to the solutions of each case (Figure 2). The curve equations represent constraints on the optimisation problem.

COSTING

The cost of the structure in this study, consists of the cost of the materials in the composite section (concrete and reinforcement), plus formwork:

$$C_s=V_c C_c+ V_r C_r+ A_f C_f \tag{22}$$

where, C, V are cost and volume, respectively, s stands for structure, c for concrete r for reinforcement and f for formwork. Typical reinforcement costs can be found in Table 1. The numbers in the last column refer to the cost of carrying 1 MN failure load per meter length of bar. Concrete cost in £ sterling for the southern parts of UK follows the formula: $C_{concrete}=37.25e^{0.006fc}$ where f_c is in MPa.

Table 1: Reinforcement cost

Material	**Price** £/kg	**Density** (gr/cm^3)	**Price** £/(MN*m)
Steel	0.38	7.8	8.6478
Glass	3.75	2.5	10.4
Aramid	12.5	1.45	12.94
Carbon	10.625	1.7	8.2102

RESULTS

The principles given above were applied to a typical simply supported beam structure. The beam had a clear span of 6m and a cross section as shown in Figure 1. The web was 0.2m wide and the flange 0.1m thick. It supports a square 5m-side and 0.1m-thickness slab. The slab loads the beam with its own weight and a 2 kN/m^2 live load. The beam is reinforced with steel, glass (GFRP), aramid (AFRP) or carbon (CFRP). Their properties can be found in Table 2.

Table 2: Reinforcement properties

	Steel	GFRP	AFRP (Fibra)	CFRP
Strength (MPa)	460	900	1480	2200
Elastic Modulus (GPa)	210	40	68.6	130
Failure Strain	0.1	0.022	0.02	0.013

In Figure 2, typical plots of reinforcement area versus section depth for steel, GFRP, AFRP and CFRP are shown. Concrete strength was 40 MPa and the partial material safety factors: concrete 1.5, steel 1.15, GFRP 1.3, and CFRP-AFRP 1.15 (Eurocrete, 2000). For long term deflection calculations $\chi\varphi$ was taken as 3. Shrinkage strain was 0.0003. The compression strain limit was set to 0.001. The crack width was limited to 0.3mm. The surface of the FRPs was assumed to be braided and sanded, with bond properties: N=0.251, τ_1=17.78 MPa, s_1=0.15 mm, τ_2=7.13 MPa and s_2=0.24 mm (Cosenza et al., 1997). For steel, bond properties

were taken from pull-out tests recently completed for Confibrecrete: N=0.3, τ_1=25 MPa, s_1=0.7 mm, τ_2=15 MPa and s_2=1.3 mm.

Each design constraint is shown in Figure 2 as functions of section depth and area of reinforcement. They lead to a feasible zone for the beam where all the constraints are satisfied. The costing function is also shown in the graph; it is linear and its slope depends on the relative cost of the concrete and reinforcement. The cost slope, for the same concrete strength, is lowest for steel and increases for GFRP, CFRP and AFRP respectively. The optimum solution is located at the point where the costing function first meets the design feasible zone. For steel-RC beam this occurs at the intersection between ultimate and deflection constraint. On the other hand, for FRP-RC beams, the optimum point is at the deflection – minimum reinforcement ratio intersection. It can also be observed that for lower bar stiffness the working constraints move upwards to satisfy the design limits. So for GFRP, which has the lowest stiffness, the beam should be around 0.75m depth and 1350mm^2 bar area, to satisfy the deflection condition, while failing with crushing of concrete at ultimate.

A parametric study was carried out to study the effect of various design parameters on the optimum solution and the results in terms of cost can be found in figure 3. For each material all optimum solutions were formed by 2 or more design constraints coming both from ultimate and working load conditions. For steel the ultimate condition was always the

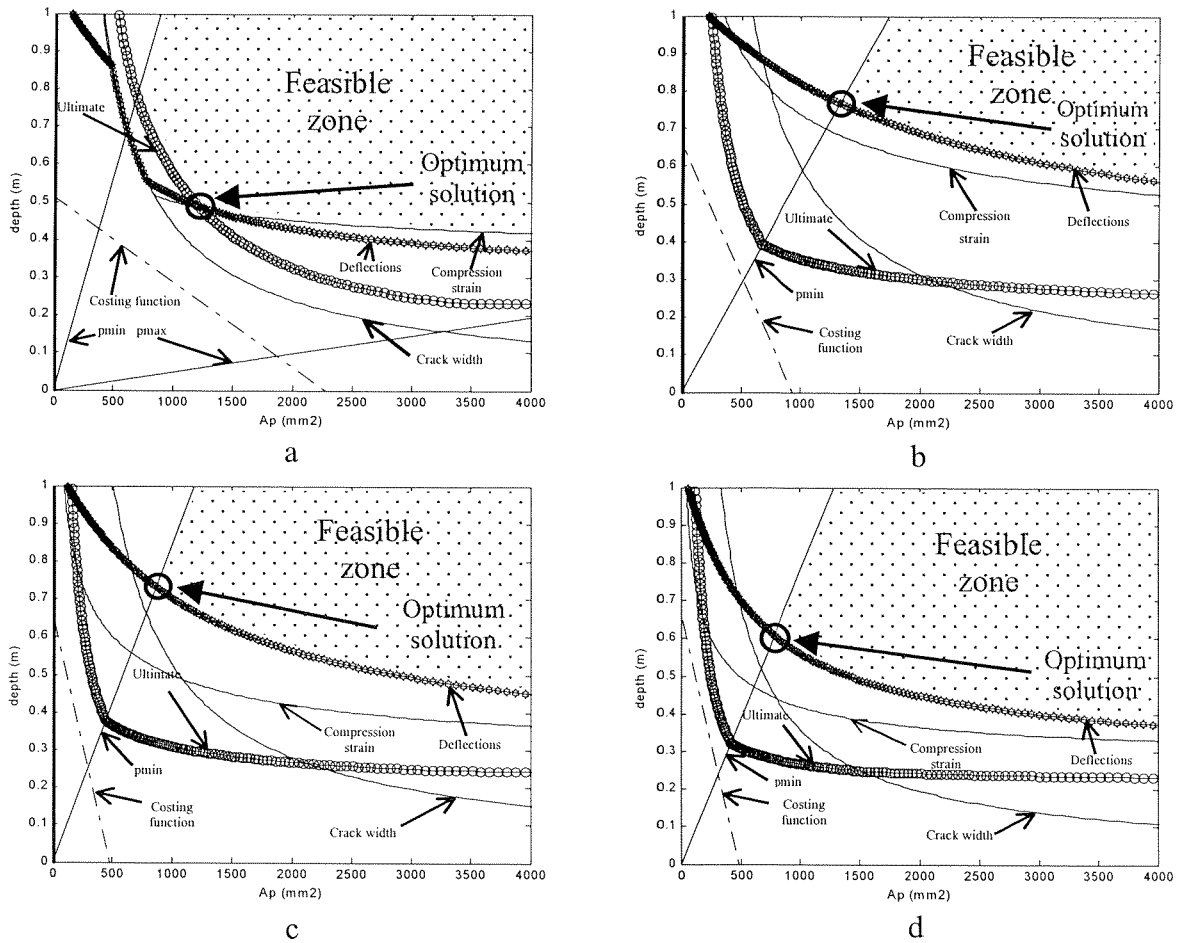

Figure 2: Depth versus area of reinforcement diagrams for: a. steel b. GFRP c. AFRP, d. CFRP reinforced concrete beams.

strength limit, combined with one of the deflections, compression strain or crack width conditions. In the same way, for FRPs the ultimate condition was always the minimum reinforcement ratio constraint, followed by one or more working constraints.

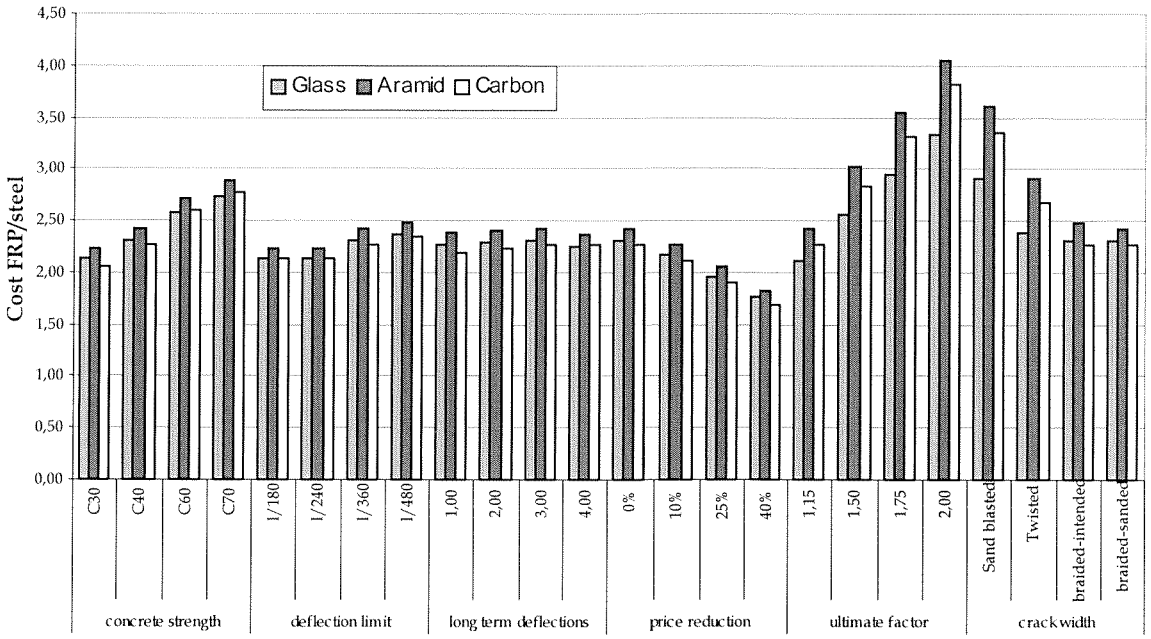

Figure 3: Optimum costs of structures reinforced with glass, aramid and carbon bars, for various design parameters

The partial material safety factor gave a substantial increase in the cost of all FRP reinforced beams. The minimum reinforcement constraint depends directly on the strength of the bars. For high partial material safety factors the slope of the minimum reinforcement constraint requires greater FRP areas which significantly increased the final cost, because FRPs are expensive.

If it is assumed that FRP costs will reduce, the cost of the structure reduces but the optimum beam dimensions are the same. FRP costs have to reduce by very significant amounts before the optimum dimensions change.

Increasing the concrete strength to reduce deflections in FRP design, does indeed work by reducing the beam depth, but the cost increases because for higher strength concrete more reinforcement is needed to avoid snapping of bars. Similarly, if strict deflection limits are applied the cost increases; beam depth also increases to the value, which depends on the bar stiffness.

Ratios of FRP/steel RC beams costs are shown in Table 3 for various spans and section shapes. The ratios increase with greater spans, due to higher deflections. But a heavy infuence on cost is observed when increasing top flange width. Bars are stressed to higher levels to balance the increasingly high concrete compression area.

To study the influence of the crack width on the cost four different bars with different surface configurations were introduced: twisted, sand blasted, braided-indented and braided-sanded (Table 4).

Table 3: Optimum costs of reinforced beams with various spans and section shapes (bar surface: braided and sanded).

Case	Parameter value	Glass				aramid				carbon				steel		
		Ap (mm^2)	depth (m)	Cost (£/m)	Cost glass/steel	Ap (mm^2)	depth (m)	Cost (£/m)	Cost aramid/steel	Ap (mm^2)	depth (m)	Cost (£/m)	Cost carbon/steel	Ap (mm^2)	depth (m)	Cost (£/m)
span	3.50	1113	0,41	19,2	2,11	621	0,41	20,1	2,21	632	0,34	19,3	2,13	710	0,29	9,09
	4.50	1426	0,52	23,8	2,20	795	0,53	24,9	2,31	774	0,44	23,3	2,16	912	0,37	10,79
	5.50	1739	0,64	28,3	2,27	969	0,65	29,7	2,38	943	0,54	27,8	2,22	1110	0,45	12,49
	7.00	2229	0,81	35,4	2,34	1242	0,82	37,2	2,46	1209	0,69	34,6	2,30	1383	0,58	15,09
flange width	rectangular	975	1,08	24,3	1,83	533	1,10	25,1	1,88	541	0,94	23,0	1,73	723	0,80	13,33
	0.40	1446	0,77	25,9	2,04	805	0,78	27,1	2,13	811	0,67	25,8	2,02	974	0,60	12,74
	0.80	2360	0,65	35,7	2,45	1317	0,66	37,6	2,58	1272	0,54	35,2	2,41	1242	0,47	14,59
	1.20	3262	0,58	46,1	2,68	1821	0,59	48, 7	2,83	1745	0,48	45, 8	2,66	1285	0,46	17,19

The crack width limit in all cases was set to 0.3mm for aesthetic reasons. The results show a significant influence of the bond surface characteristics of the bars on cost. In all cases, except the braided and sanded, the crack width governs the design. So good bond properties for FRP bars give economic solutions.

Table 4: FRP bond parameters for various surface configurations (Cosenza et al., 1997).

	N	τ_1	s_1	τ_2	s_2
Sand blasted	0.251	2.74	1.08	1.38	1.28
Twisted	0.175	4.15	0.45	3.68	0.46
Braided and intended	0.177	10.2	2.14	6.26	2.20
Braided and sanded	0.069	17.78	0.15	7.13	0.24

From Figure 3 and Table 3, it can be seen that aramids generally gave the most expensive solutions to the given problem, due to its price in comparison to its stiffness. On the other hand although glass is much cheaper than carbon, the final costs were almost equal. The low stiffness of glass, and its lower strength in comparison to carbon, pushes the working conditions to high depths and bar areas, to control the working limits and achieve the desired mode of failure. Furthermore, glass design solutions are not very practical, with relatively high section depths. Typical depths for GFRP RC beams are 1.3-1.4 that of steel. For CFRP RC beams the ratio is about 1.1-1.2. Taking into account the durability problems of glass in concrete, carbon seems to be a more attractive material for reinforced concrete applications.

CONCLUSIONS

The initial cost of RC structures with FRPs was presented. A typical structure was solved for the design cases and an optimum solution was found in terms of cost. A parametric study was carried out to identify the which parameters most affect the cost of the structure. Based on the results of this study the following conclusions are drawn:

- The optimum solutions were always governed by 2 or more constraints. The FRP structures were governed by both ultimate and working conditions. The ultimate load condition was to stop the undesirable snapping of FRP mode of failure.
- Increasing the concrete strength reduces deflections but not cost.
- Poor bond characteristics of FRPs bring the crack width design limit into play, which increases cost.

- Carbon, despite its high material cost, gave similar optimum costs as glass, but more practical design solutions.

ACKNOWLEDGEMENT
The authors wish to acknowledge the European Commission for funding the EU TMR Network "ConFibreCrete".

REFERENCES

ACI 440-96, (1996). *State-of-the-Art Report on Fiber Reinforced Plastic Reinforcement for Concrete Structures*, ACI Committee 440, American Concrete Institute, Detroit, Michigan.

Alsayed, S. H. and Al-Salloum, Y. A. (1996). Optimisation of Flexure Environment of Concrete Beams Reinforced with Fibre-Reinforced Plastic Bars, Magazine of Concrete Research, 48(174): 27-36.

Bedard, C. (1992). Composite Reinforcing Bars: Assessing their Use in Construction, Concrete International 14(1): 55-59.

Bazant, Z. (1972). Predictions of Concrete Creep Effects Using Age-Adjusted Effective Modulus Method, ACI Journal 69(4): 212-217.

CEB (Comite Euro-International du Beton) (1985). CEB Bulletin d'information No. 158-E – Manual on Cracking and Deformation, Secretariat Permanent, EPFL, Case Postale 88, Ch-1015, Lausanne.

CEB (Comite International du Beton) (1990). *CEB-FIP Model Code 1990,* CEB Bulletin d'Information 213-214, Thomas Telford Service Ltd., London.

Cosenza, E., Manfredi, G. and Realfonzo, R. (1997). *Behaviour and Modelling of Bond of FRP Rebars to Concrete.* ASCE Journal of Composites for Construction.1(2): 40-51.

Eurocrete (2000). *Design Recommendations of FRP Reinforced Concrete Structures*, First Draft, Riga, Latvia.

Fickelhorn, M. (1990). *Editorial*, Materials and Structures Journal, RILEM 23(137): 317.

Heyman, J. (1982). *The Masonry Arch*, Ellis Horwood, Chichester.

Makhtouf, H. M, Abmadi, B. H. and Al-Jabal, J. (1991). *Preventing Reinforced Concrete Deterioration in the Arabian Gulf*, Concrete International 13(5): 65-67.

Stratford, T. J. (2000). *The Shear of Elastic FRP Reinforcement*, PhD Thesis, University of Cambridge.

Yang X., Nanni A. and Chen G. (2001). *Effect of Corner Radius on the Performance of Externally FRP Reinforcement*, Fifth International Symposium on Fibre Reinforced Plastics for Reinforced Concrete Structures (FRPRCS-5), Burgoyne C. J. (ed.): 197-204.